Cellulose (2022) 29:8085–8101
https://doi.org/10.1007/s10570-022-04770-9

ORIGINAL RESEARCH

Insights into characteristics and thermokinetic behavior of potential energy-rich polysaccharide based on chitosan

Ahmed Fouzi Tarchoun · Djalal Trache · Mohamed Abderrahim Hamouche · Wissam Bessa · Amir Abdelaziz · Hani Boukeciat · Slimane Bekhouche · Djamal Belmehdi

Received: 23 May 2022 / Accepted: 20 July 2022 / Published online: 6 August 2022

Abstract To explore polysaccharides for developing energetic biopolymers, a promising energy-rich nitrochitosan (NCS) was successfully prepared through electrophilic nitration of chitosan. The chemical structure and morphology of the synthesized NCS and its precursor were confirmed by infrared spectroscopy, elemental analysis, and scanning electron microscopy. The energetic performance, thermal behavior, and degradation kinetics of NCS were also evaluated. The results showed that the designed nitrogen-rich (Nc = 16.79%) NCS presents excellent energetic features, such as a calorific value of 10,573 J/g, a density of 1.708 g/cm^3, an impact sensitivity of 15 J, and a detonation velocity of 7788 m/s, which are markedly better than those of NC and GAP. Meanwhile, the thermal investigation based on deconvoluted non-isothermal DSC experiments combined with isoconversional kinetic methods indicated that NCS displays two consecutive exothermic decomposition events within the temperature range of 133–180 °C and 185–240 °C, and exhibits apparent activation energies of 74 kJ/mol and 152 kJ/mol, respectively, which are lower than the common thermolysis energy range of NC (140–190 kJ/mol), demonstrating the improved reactivity of the aforementioned energetic NCS. Overall, this study established that NCS could serve as an outstanding energetic polysaccharide for potential application in high-performance composite explosives and solid rocket propellants.

Keywords Chitosan · Nitration · Energetic polymers · Thermal kinetics · Detonation performance

A. F. Tarchoun (✉) · D. Trache (✉) · M. A. Hamouche · W. Bessa · A. Abdelaziz · H. Boukeciat · S. Bekhouche
Energetic Materials Laboratory, Teaching and Research Unit of Energetic Processes, Ecole Militaire Polytechnique, BP 17, Bordj El-Bahri, 16046 Algiers, Algeria
e-mail: tarchounfouzi@gmail.com

D. Trache
e-mail: djalaltrache@gmail.com

A. F. Tarchoun · D. Belmehdi
Energetic Propulsion Laboratory, Teaching and Research Unit of Energetic Processes, Ecole Militaire Polytechnique, BP 17, Bordj El-Bahri, 16046 Algiers, Algeria

Introduction

In today's age, the valorization of natural materials for the development of renewable energy technologies has been prioritized worldwide to reduce the excessive consumption of ever-depleting fossil fuels and the environmental hazards associated with their processing (Peter et al. 2021; Reshmy et al. 2022; Tarchoun et al. 2022c). In this regard, polysaccharides have been revealed to be promising candidates and have already dominated research revolving around the design of new biobased products (Mohammed et al. 2021; Nasrollahzadeh et al. 2021). Among those of interest, chitosan (CS) is the second natural polysaccharide after cellulose in terms of abundance,

distribution, and usage (Joseph et al. 2021; Negm et al. 2020; Sivanesan et al. 2021).

From the production point of view, CS is commonly prepared through alkaline deacetylation of chitin derived from crustaceans and shrimp shells (Blilid et al. 2020; Huet et al. 2021; Mujtaba et al. 2020). The hierarchical molecular structure of CS is typically constituted by repeating β-(1,4)-linked D-glucosamine units encountered with one primary amine (NH_2) linked to the C2 carbon and two hydroxyl groups (OH) bonded to the C3 and C6 carbons (Bakshi et al. 2020; Farkas et al. 2020). These free reactive amino functions are mainly responsible for the greater chemical and functional features of CS compared with chitin. Furthermore, the structure of CS is similar to that of cellulose, with the major difference being the replacement of the OH group at the C2 position of cellulose by a primary amino function in CS.

This carbohydrate biopolymer, in addition to being biodegradable and renewable, displays outstanding features such as non-toxicity, biocompatibility, good thermal stability, great chemical reactivity, and the ability to modify its surface functionality, offering opportunities to develop innovative materials with advanced functionalities (Mujtaba et al. 2020; Negm et al. 2020; Rabiee et al. 2022). Recently, CS has captured tremendous considerable interest from the scientific community as a promising nitrogen-rich polysaccharide for practical use in widespread areas including food packaging, water treatment, medicine, and biofuel, to name a few (Oladzadabbasabadi et al. 2022; Rezaei et al. 2021; Yin et al. 2021). However, the search for new applications and improving the properties of the current CS-based products are crucial driving forces for the development of the next generation of CS derivatives.

In the field of polysaccharides-derived energetic substances, nitrocellulose (NC) is still the most well-known and widely employed energy-rich biopolymer in a diverse range of military and industrial areas owing to its beneficial properties (Tarchoun et al. 2022a; Trache and Tarchoun 2019). Nevertheless, numerous researchers have demonstrated that the futuristic energetic cellulose-rich biopolymers and their practical utilization in advanced formulations cannot simply be reached using the traditional NC (Dobrynin et al. 2019; Tarchoun et al. 2021c). For instance, it was highlighted in our recent papers that chemical functionalization and physical downscaling of pristine cellulose are very powerful approaches to developing new insensitive and high-energy dense biopolymers, such as carbamated-microcrystalline cellulose nitrate (Tarchoun et al. 2021b; Tarchoun et al. 2021d), aminated microcrystalline cellulose nitrate (Tarchoun et al. 2020a, 2020c), and nitrated tetrazole-acetate-functionalized cellulose microcrystals (Tarchoun et al. 2021a, 2020b). Therefore, these outstanding findings on high-energy cellulosic biopolymers have motivated us to explore other alternative biopolymers, mainly chitosan, to design a new generation of energetic nitrogen-rich polysaccharides for potential use in advanced energetic formulations.

Based on the open literature, there are only a few research papers dealing with the nitration of chitosan to obtain energetic nitrochitosan (NCS) (Hirano and Yano 1986; Jha et al. 2013; Poli et al. 2015; Zeng et al. 2005). In one recent investigation, Rahman et al. reported the synthesis of O-nitrated chitosan with a low nitration level for use as electrolyte biopolymer in electrochemical devices (Rahman et al. 2019). More recently, Li and coworkers were the first authors who prepared highly nitrated chitosan with an improved energetic performance and mentioned its great potential application in solid propellants (Li et al. 2020). However, the non-isothermal decomposition behavior and chemical kinetics of such nitrogen-rich biopolymer have not been investigated so far. Therefore, the determination of the kinetic parameters of the as-prepared NCS is a prerequisite and can offer excellent information to well understand its thermal runaway mechanism and accurately estimate the effect of its degradation on the potential hazard during its preparation, storage and real-world applications (Huang et al. 2019; Li et al. 2022; Liu et al. 2022). Therefore, to promote the use of energetic biopolymers and reinforce the current knowledge about their thermochemical kinetics, the aim of the present work is the synthesis of highly nitrated chitosan and scrutinize its physicochemical properties, chemical structure, morphology, mechanical sensitivities, and energetic performance. In addition, its thermal behavior is evaluated based on non-isothermal DSC experiments, followed by a deep kinetic analysis using isoconversional integral approaches to suitably evaluate its safety performance, and offer guidelines for its potential application in composite explosives and solid propellants. The obtained results were compared to those

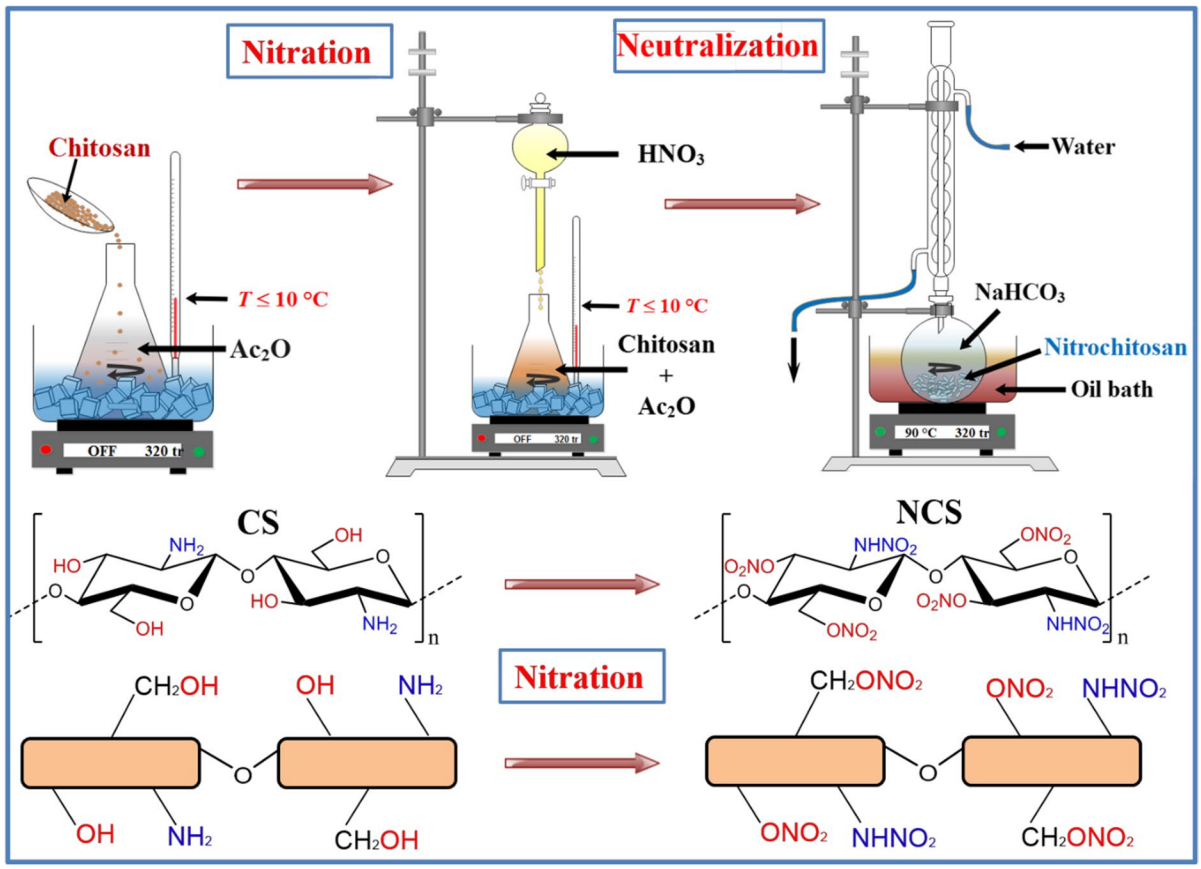

Scheme 1 Synthetic route for the preparation of nitrochitosan

of other energetic polymers reported in the literature as well.

Experimental

Materials

Chitosan with a deacetylation degree of 98% and a viscosity-average molecular weight of 100–300 kDa was purchased from Acros Organics. Acetic anhydride (Ac_2O), fuming nitric acid (HNO_3), and sodium bicarbonate ($NaHCO_3$) were acquired by VWR-Prolabo. All chemicals were utilized as received without further purification. Nitrocellulose, with a nitrogen content of 12.61%, was previously prepared at EMLab as reported in our previous paper (Tarchoun et al. 2020a), and it was used as a reference sample.

Synthesis of nitrochitosan

Nitrochitosan was prepared through electrophilic nitration of chitosan precursor, following the typical methodology mentioned by Li et al. with slight modifications (Li et al. 2020). As depicted in Scheme 1, the dried CS (1 g) was firstly added in small portion into Ac_2O (7 mL), followed by dropwise addition of fuming HNO_3 (7 mL) under mechanical stirring. The nitration reaction was performed in an ice bath ($T \leq 10$ °C) for 5 h under strong magnetic stirring. After soaking the reaction by slowly adding cold water, the residue was filtered and treated with boiled $NaHCO_3$ (2%, w/v) for 2 h, then with boiled water for 2 h. The neutralization process was carried out in triplicate, and the resulted product was filtered, thoroughly rinsed with distilled water, and dried under a vacuum to afford the corresponding NCS. It is important to mention

that a high level of safety precautions has been taken to avoid any risk of hazardous ignition during the nitration process. Anal. found (%): C 24.93, H 2.80, N 16.79; calcd. (%): C 24.32, H 2.70, N 18.92.

Characterization techniques

Density, nitration level, and sensitivity assessments

Experimental densities of the starting CS and its nitrated derivative were determined using an automatic true density meter, type Accupyc 1340 II pycnometer. Ten measurements were achieved at 25.4 ± 0.5 °C, which served to calculate the mean density and standard deviation.

Elemental characterization was carried out in a Vario III Elemental analyzer to quantify the nitrogen content of the synthesized NCS and its CS precursor. The experiments were performed in triplicate, and the average value was reported.

The impact (IS) and friction (IF) sensitivities of NCS were measured according to the STANAG 4489 and STANAG 4487 by employing a standard BAM drop hammer and friction tester, respectively (UN-TDG, UN 2009). The limiting impact energy was obtained as the lowest energy at which a positive result, which is characterized by an audible report, crackling, sparking, or a flame, was obtained from at least one out of six repeated trials. Besides that, the lowest force at which a positive result, recorded as the limiting friction sensitivity, is obtained from at least one out of six repeated trials.

Structural analyses

Fourier transform infrared (FTIR) spectra were recorded using a Perkin Elmer 1600 spectrometer collected in ATR mode at room temperature with a resolution of 1 cm^{-1} by co-adding 64 scans for each spectrum in the range from 4000 to 500 cm^{-1}.

To further elucidate the sample microstructure, an FEI Quanta 600 scanning electron microscope was used to examine the surface morphology of CS and NCS. The samples were coated with 20 nm of carbon and analyzed with a secondary electron detector at an accelerating voltage of 5 kV.

Thermal analysis and kinetic computations

The thermal behavior of the investigated polysaccharides was assessed, within the temperature range of 50–450 °C, by thermogravimetric analysis (TGA) and differential scanning calorimetry (DSC), using Perkin-Elmer TGA 8000 and DSC 8000 analyzers, respectively. The data were recorded under a constant dry nitrogen atmosphere (30 mL/min) for a small amount of sample (1.5–3 mg), using DSC's stainless steel high-pressure capsules for energetic samples and regular aluminum capsule for CS, at a heating rate of 10 °C/min for TGA, while at distinct heating rates (5, 10, 15 and 20 °C/min) for DSC. The uncertainties associated with the thermal properties were evaluated based on repeated measurements (threefold) and found to be within ± 0.1 K for the decomposition and 10 J/g for the enthalpy.

The DSC data were subjected to isoconversional kinetic analysis following the recommendation of the International Confideration for Thermal Analysis and Calorimetry (ICTAC) to evaluate the dependence of the kinetic triplet, namely, the activation energy (E_a), the pre-exponential factor (*Log (A)*) and the mechanism of thermal decomposition ($g(\alpha)$) with the conversion (α) (Vyazovkin et al. 2020). The value of α is calculated as a ratio of the current heat change ΔH to the total reaction heat ΔH_{total}:

$$\alpha = \frac{\int_{t_0}^{t} \left(dH/dt\right) dt}{\int_{t_0}^{t_f} \left(dH/dt\right) dt} = \frac{\Delta H}{\Delta H_{total}} \tag{1}$$

Linear isoconversional models, namely, Trache-Abdelaziz-Siwani (TAS) (Trache et al. 2017), and the iterative Kissinger–Akahira–Sunose (it-KAS) (Trache et al. 2018), were applied to determine the kinetic triplet (E_a, *Log* (*A*), $g(\alpha)$). These approaches are based on an approximate form of the temperature integral:

$$g(\alpha) = \int_0^{\alpha} \frac{d\alpha}{f(\alpha)} = \frac{A}{\beta} \int_{T_0}^{T} e^{-E_a/RT} dT \tag{2}$$

In addition to the above-mentioned models, the dependence of the E_a with α was evaluated using a non-linear isoconversional Vyazovkin's method (VYA) (Sbirrazzuoli 2020). This approach uses a numerical algorithm, and the E_a is found as the value that minimizes the objective function:

$$\Phi(E_\alpha) = \sum_{i=1}^{n} \sum_{j \neq i}^{n} \frac{I(E_\alpha, T_{\alpha,i})\beta_j}{I(E_\alpha, T_{\alpha,j})\beta_i} \quad (3)$$

$$I(E_\alpha, T_{\alpha,i}) = \int_0^{T_{\alpha,i}} e^{\left[-\frac{E_\alpha}{RT}\right]} dT \quad (4)$$

To complete the determination of the kinetic triplet, the compensation effect approach (CE) was used to predict the frequency factor and the reaction model. The computation was performed using a local code compiled in MATLAB software. More details about the followed kinetic modeling can be found elsewhere (Benhammada et al. 2020; Chelouche et al. 2019; Trache et al. 2017).

Energetic performance

In order to evaluate the energetic features of the prepared NCS, its heat of combustion (ΔU_{comb}) was firstly determined with a Parr 6200 bomb calorimeter under an oxygen pressure of 30 bar. The obtained results represent the average of three separate measurements. The obtained ΔU_{comb} was then used to calculate the standard enthalpy of combustion (ΔH_{comb}) and formation (ΔH_f) based on the Hess thermochemical cycle and combustion reaction. The theoretical energetic performance parameters, including detonation parameters and specific impulse of the developed NCS, were also predicted by the EXPLO5 thermodynamic code version 6.04 based on its experimental density and calculated enthalpy of formation (Sućeska 2017).

Results and discussion

Physicochemical features and mechanical sensitivity

NCS was synthesized through electrophilic substitution of hydronium ions (H^+) of reactive hydroxyl and amino groups of the CS bridge structure with nitronium ones (NO_2^+) formed in the nitration medium, as illustrated in Scheme 1. A preliminary experiment showed that the nitration of CS with the concentrated sulfonitric mixture, commonly used to prepare NC, furnishes a high viscous solution and the reaction products cannot be separated, which is probably caused by protonation of the amino function by the sulfuric acid leading to ionization of CS as a consequence. This problem has been smoothly addressed by replacing sulfuric acid with acetic anhydride. The whole nitration process can be divided into two steps: (1) Ac_2O, as a strong dehydrating agent, interacts with the OH and NH_2 sites of glucosamine units and increases their nucleophilicity; (2) with the assistance of Ac_2O as a catalyst, the released electrophilic NO_2^+ from fuming HNO_3 are easily attracted by the stabilized and highly reactive OH and NH_2 to form explosophoric nitrate ester (O-NO_2) and nitramine (NH-NO_2), respectively.

The determined results of density (ρ) and nitrogen content (Nc) for CS and its energetic NCS derivative are listed in Table 1. For comparison purposes, these parameters of NC, microcrystalline cellulose nitrate (MCCN), and glycidyl azide polymer (GAP) are also included. As can be revealed, the synthesized NCS exhibits improved density (1.708 g/cm^3) and nitration level (16.79%) compared to its CS precursor, certifying the effective nitration process. Those values are slightly higher than those of highly nitrated chitosan (ρ of 1.70 g/cm^3 and Nc of 16.67%) prepared in previous work

Table 1 Physicochemical properties and mechanical sensitivities

Sample	Nitrogen content (%, w/w)	Density (g/cm^3)	Impact sensitivity (J)	Friction sensitivity (N)
CS	8.02 ± 0.04	1.546 ± 0.002	–	–
NCS	16.79 ± 0.03	1.708 ± 0.003	15	> 360
NC (Tarchoun et al. 2020a)	12.61 ± 0.02	1.671 ± 0.002	3	350
MCCN (Tarchoun et al. 2021d)	13.08 ± 0.03	1.694 ± 0.004	2	350
GAP (Wu et al. 2020)	42.42	1.30	8	324

(Li et al. 2020). Furthermore, Compared to the conventional NC and emergent MCCN, the actual physicochemical properties of NCS are markedly better, demonstrating the greater advantages of using CS as starting polysaccharide rather than pristine cellulose to develop promising nitrogen-rich biopolymer for futuristic energetic applications. It is also interesting to point out that the experimentally determined density of the designed NCS is much higher than that of the commonly known energetic binders such as GAP (1.30 g/cm^3) (Wu et al. 2020), and poly(glycidyl nitrate) (Poly GLYN: 1.46 g/cm^3) (Yan et al. 2016), and surpass those of some recently developed energetic poly(ionic liquids) (1.60–1.65 g/cm^3) (Wang et al. 2018).

On the other hand, to evaluate the safety performance of the developed NCS, its impact and friction sensitivities (*IS* and *FS*) are determined, and the tested results are reported in Table 1. It is obvious that NCS is friction insensitive, whereas, it presents relatively impact insensitivity similar to that of TNT explosive (*IS* = 15 J) (Tang et al. 2020), but interestingly greater than the currently used energetic NC (*IS* = 3 J) and GAP (*IS* = 8 J) polymers (Tarchoun et al. 2020d). Above all, NCS, as an emergent energetic nitrogen-rich biopolymer, shows its great potential to be employed in the near future to develop new high-energy dense formulations and composite explosives due to its excellent physicochemical performance.\

Chemical structure and morphology

The chemical functionalities of the starting CS and its nitrated derivative (NCS) were identified by FTIR analysis, and the recorded spectra are illustrated in Fig. 1, also including the IR spectra of NC for comparison. As can be perceived, NCS and its CS precursor display the characteristic absorbance bands of glucosamine unit, such as O–H stretching at 3360 cm^{-1}, N–H stretching at 3280 cm^{-1}, C-H stretching at 3900 cm^{-1}, intra- and intermolecular hydrogen bonding at 1650 cm^{-1}, N–H bending at 1580 cm^{-1}, CH_2 bending at 1380 cm^{-1}, C–N stretching at 1320 cm^{-1}, C–O–C stretching of pyranose ring at 1160 cm^{-1}, and ß-1,4-glycosidic linkage vibration at 890 cm^{-1} (Mauricio-Sánchez et al. 2018; Mohan et al. 2020; Pinto et al. 2021). It can be also deduced from Fig. 1 that the obvious structure alterations that raised after nitration is related to the significant drop in the intensity of O–H and N–H peaks, and the clear appearance of the typical vibrational bands of energetic NO_2, N-NO_2, and O-NO_2 groups in the fingerprint region from 1800 cm^{-1} till 500 cm^{-1}. In addition, the molecular structure of NCS is found to be similar to that of NC, with the most detailed difference being the presence of the weak N–NO_2 vibrational band at 1426 cm^{-1} for NCS (Li et al. 2020; Tarchoun et al. 2022b). These findings provide evidence for the effective nitration pathway without destruction of the main polysaccharide skeleton and confirm the successful chemical structure of the desired energetic NCS biopolymer.

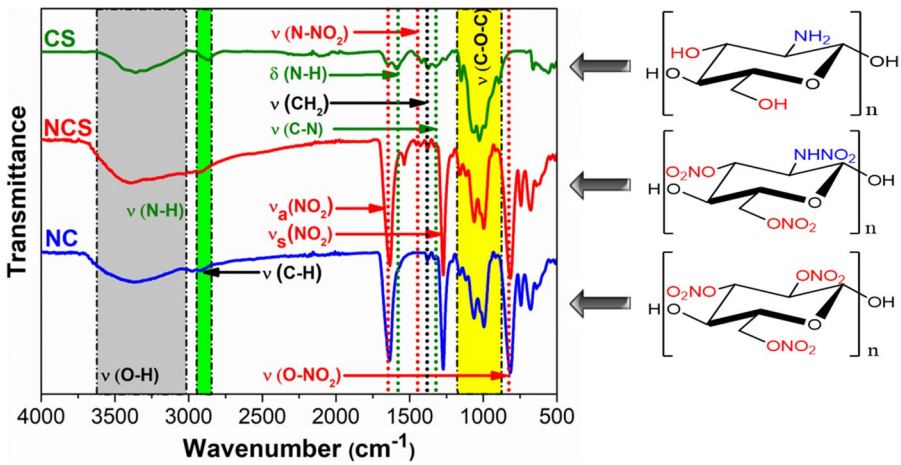

Fig. 1 **a** FTIR spectra of chitosan, nitrochitosan and nitrocellulose

The microstructure of pristine CS and its NCS derivative was also examined using SEM analysis to investigate the eventual morphological alterations caused by the electrophilic nitration. Figure 2 illustrates the lateral surface micrographs of CS, NCS, and NC. As noticed, NCS shows the same granular structure shape as its CS precursor, indicating homogenous esterification with uniform distribution of NO_2 groups and negligible influence on the main microstructure. However, a rough surface, rather than a clear and smooth one for CS, is noted for NCS, which is attributed to the inserted electron-withdrawing O–NO_2 and N–NO_2 groups that cover the surface of glucosamine units. Similar findings of the morphological structure of CS-based materials are reported elsewhere (Ahmad et al. 2022; da Silva Lucas et al. 2021; Rasweefali et al. 2021).

For comparison, the morphological structure of previously studied cellulose and NC is also reported in Fig. 2. We can clearly reveal that, contrary to the morphology of the investigated CS-based biopolymers, the common NC and its cellulose precursor present a fibrous aspect with long individualized filaments (Nikolsky et al. 2019; Tarchoun et al. 2022a). This discrepancy in visual morphology and physical state of the surface between CS and cellulosic polysaccharides might be attributed to the difference in organisms from which they originate and the hydrogen-bonding systems (Mohan et al. 2020; Nasrollahzadeh et al. 2021). Besides that, it is important to notice that the rounded shape of the developed NCS could be the reason for its superior physicochemical features and promote its potential use in the energetic field.

Thermal behavior

In order to evaluate the suitability and real-world use of the developed energetic NCS, its thermal stability and decomposition behavior were studied by TGA and DSC, and the acquired thermograms and thermal parameters are depicted in Fig. 3 and Table 2,

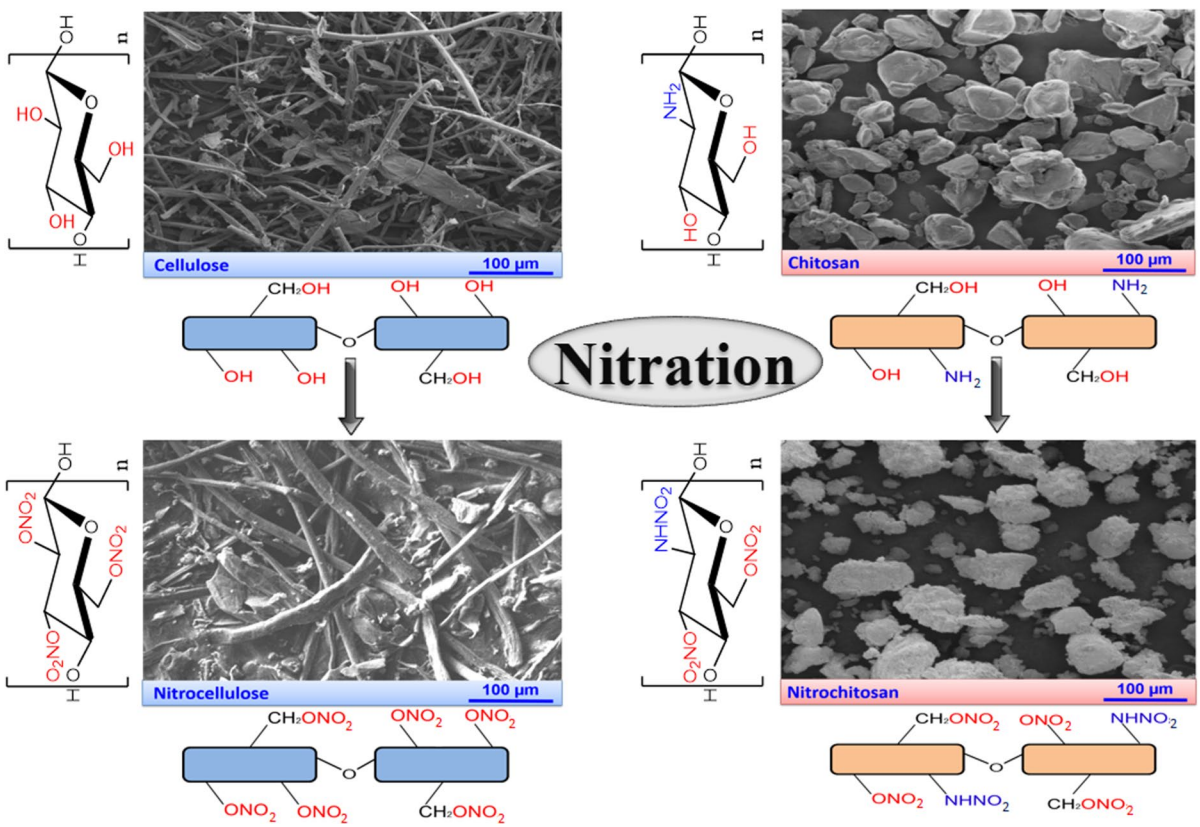

Fig. 2 SEM micrographs of chitosan, cellulose, and their nitrated derivatives

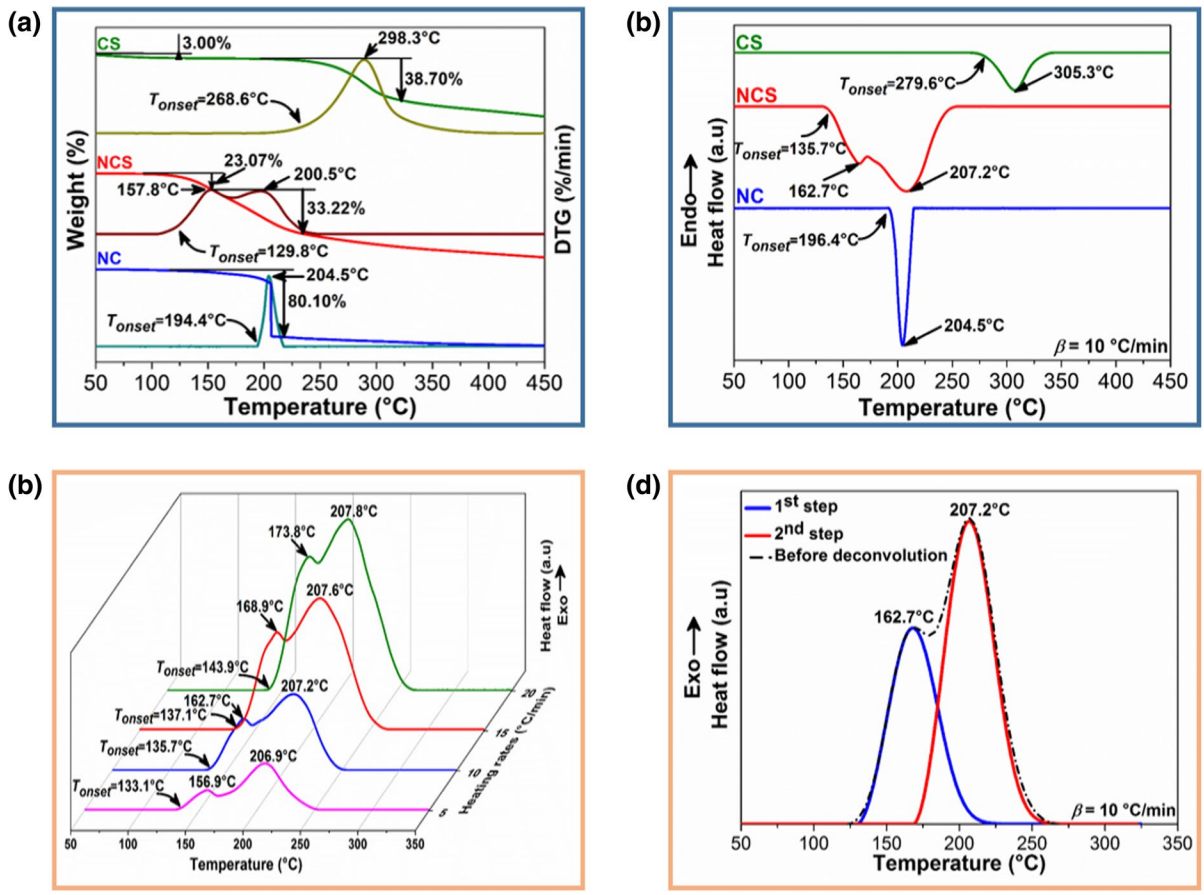

Fig. 3 **a** TGA/DTG and **b** DSC thermograms of chitosan, nitrochitosan and nitrocellulose at β = 10 °C/min; **c** Non-isothermal DSC curves of nitrochitosan; **d** Peak deconvolution of DSC curve at a heating rate of 10 °C/min

Table 2 TGA/DTG and DSC parameters of the investigated biopolymers obtained at $\beta = 10$ °C/min

Sample	TGA/DTG					DSC				
	T_{onset} (°C)	T_{peak1} (°C)	T_{peak2} (°C)	T_{endset} (°C)	Δm_T (%)	T_{onset} (°C)	T_{peak1} (°C)	T_{peak2} (°C)	T_{endset} (°C)	ΔH_T (J/g)
CS	268.6	298.3	–	322.6	38.70	279.6	305.3	–	330.0	− 785
NCS	129.8	157.8	200.5	234.4	56.29	135.7	162.7	207.2	242.7	− 2285
NC	194.4	204.5	–	217.9	80.10	196.4	204.5	–	215.1	− 1545

respectively. It should be mentioned that TGA is a common technique for measuring the relationship between mass and temperature, whereas DSC is one of the most frequently applied thermal analysis instruments, which has extremely high sensitivity and temperature resolution and can test the weakest thermal effects (Huang et al. 2021a; Huang et al. 2021b; Zhou et al. 2022). As observed from the TGA/DTG curves given in Fig. 3a, the raw material (CS) underwent two mass loss processes. The first one, accompanied by a very small weight loss (3.00%), is corresponded to the evaporation of absorbed moisture that occurs in the temperature range of 70–120 °C (Kahdestani et al. 2021; Mohan et al. 2020). The second stage, which happens with an important weight loss of approximately 38.70% recorded in the range of 230–340 °C, represents the degradation of CS framework through multiple processes such as depolymerization,

decarboxylation, and thermolytic cleavage of glycosidic bonds followed by the formation of charred residue (da Silva Lucas et al. 2021; Peter et al. 2021). After nitration, the formed NCS presents two overlapped stages of decomposition with mass losses of 23.07% and 33.22% observed at maximum peak temperatures of 157.8 °C and 200.5 °C, respectively, which agreed well with the thermal behavior of high-substituted nitrochitosan reported in the literature (Zhang et al. 2022). This outcome indicates that NCS did not decompose completely at its ignition temperature. Moreover, it is clear from Table 2 and Fig. 3a that NCS has lower thermal stability than raw CS and the common NC, but its decomposition temperature is fundamentally acceptable. This result is expected due to its increased nitration level and the presence of both energetic and thermally unstable O–NO_2 and N–NO_2 groups that significantly increase its sensitivity against thermal stimuli (Min and Park 2009; Tarchoun et al. 2021c).

Figure 3b shows the measured heat flow curves of the investigated chitosan biopolymers together with the common nitrocellulose at a heating rate of 10 °C/min. The CS thermal behavior exhibits a small exothermic peak that appeared at onset and maximum temperatures of 279.6 °C and 305.3 °C, respectively, which is related to the degradation of pyranose rings along the polysaccharide backbone (Barbosa et al. 2019; Kaya et al. 2018). NCS, however, displays two consecutive exothermic processes within the range of 133–180 °C and 185–240 °C, respectively, with a total decomposition enthalpy (ΔH_T), determined by integrating the area under the two exothermic peaks, of −2285 J/g as it is summarized in Table 2. The first degradation phenomenon that takes place at a lower temperature than that of NC is assigned to the thermolytic cleavage of the weakest N–NO_2 and O–NO_2 groups followed by the formation of highly reactive oxidizing products (Li et al. 2021; Tarchoun et al. 2020a). The second one centered at 172.3 °C has corresponded to the furtherer thermo-oxidative destruction of nitrated glucosamine units. Therefore, compared to the TGA/DTG findings, similar thermal degradation behavior is obtained by DSC.

Non-isothermal decomposition of NCS at different heating rates ($\beta = 5$, 10, 15, and 20 °C/min) has been also investigated for which the results at each β are plotted in Fig. 3c. An interesting aspect that one can depict is the shift of the two overlapping exothermic peaks towards higher temperature ranges as the heating rate increases. This expected behavior is due to the fact that faster β decreases the reaction time and delays the decomposition process (Tarchoun et al. 2021d; Wei et al. 2021). Besides that, it is worth noting that the developed NCS, in addition to its high nitrogen content, presents a basically acceptable thermal stability and much greater heat release than the conventional cellulose nitrate (1545 J/g) (Tarchoun et al. 2020a), suggesting its superior performance for future applications in the field of propulsion and explosives.

Evaluation of the thermal decomposition kinetics

For a better understanding of the thermal stability and degradation process of the developed energetic nitrogen-rich NCS, the heat flow data obtained from the DSC thermograms in Fig. 3c have been further exploited for the prediction of its key kinetic factors, i.e., the most probable reaction model and the Arrhenius parameters. Considering the two overlapped DSC peaks of NCS, the overall decomposition process was deconvoluted into two individual contributing reactions based on the asymmetric Frazer-Suzuki function, which is the most recommended method to greatly fit the multistep kinetic behaviors (Ambekar and Yoh 2018; El Hazzat et al. 2020; Hu et al. 2016; Muravyev et al. 2019). Therefore, Fig. 3d shows an example of the deconvolution of the overlapped DSC peaks, and the experimental data are well matched at all β with a high correlation coefficient ($R^2 > 0.98$). More details about the deconvolution procedure followed in this part can be found in our recent paper (Bekhouche et al. 2021).

As recommended by the ICTAC, three isoconversional kinetic approaches (TAS, it-KAS and VYA/CE) were further applied to the corresponding separated peaks in order to estimate the kinetic triplet for each step. Unfortunately, the thermal degradation kinetics of the developed energetic NCS has not yet been studied elsewhere, which makes it impossible for any attempt to compare the predicted kinetic results with those of the literature. However, structurally similar energetic biopolymers, mainly cellulose nitrate, may provide an idea of the thermokinetic process followed by the investigated NCS.

The dependency of the Arrhenius parameters (E_a and $Log\ (A)$) versus the conversion degree (α)

for each decomposition step is presented in Fig. 4, whereas Table 3 provides the average values of these parameters with their related confidence intervals and the most probable model of decomposition ($g(\alpha)$) for each process together with the kinetic values of NC available in the literature. It is obvious that the calculated E_a and $Log\ (A)$ by the used model-free integral methods are in great accordance with each other, for each step, with a relative deviation lower than 10%, justifying the excellent consistency of the computed calculations (Vyazovkin et al. 2020). Furthermore, the high precision of the predicted Arrhenius parameters using linear models (TAS and it-KAS) can be pointed out by the strong regression coefficient higher than 0.9993.

As displayed in Fig. 4, the two deconvoluted processes show different trends of Arrhenius parameters as a function of conversion, revealing that the thermokinetic behavior of NCS follows various paths and each has its own E_a and $Log\ (A)$. For the first step, which is evaluated at an apparent E_a of about 74 kJ/mol and corresponds to the main homolytic splitting of explosophoric O–NO_2 and N–NO_2 groups, the E_a values increased as the conversion rate increased until $\alpha = 0.5$, where the E_a maintained a certain level at around a constant value of 76 kJ/mol. Such behavior demonstrates that the rate of the thermolysis process

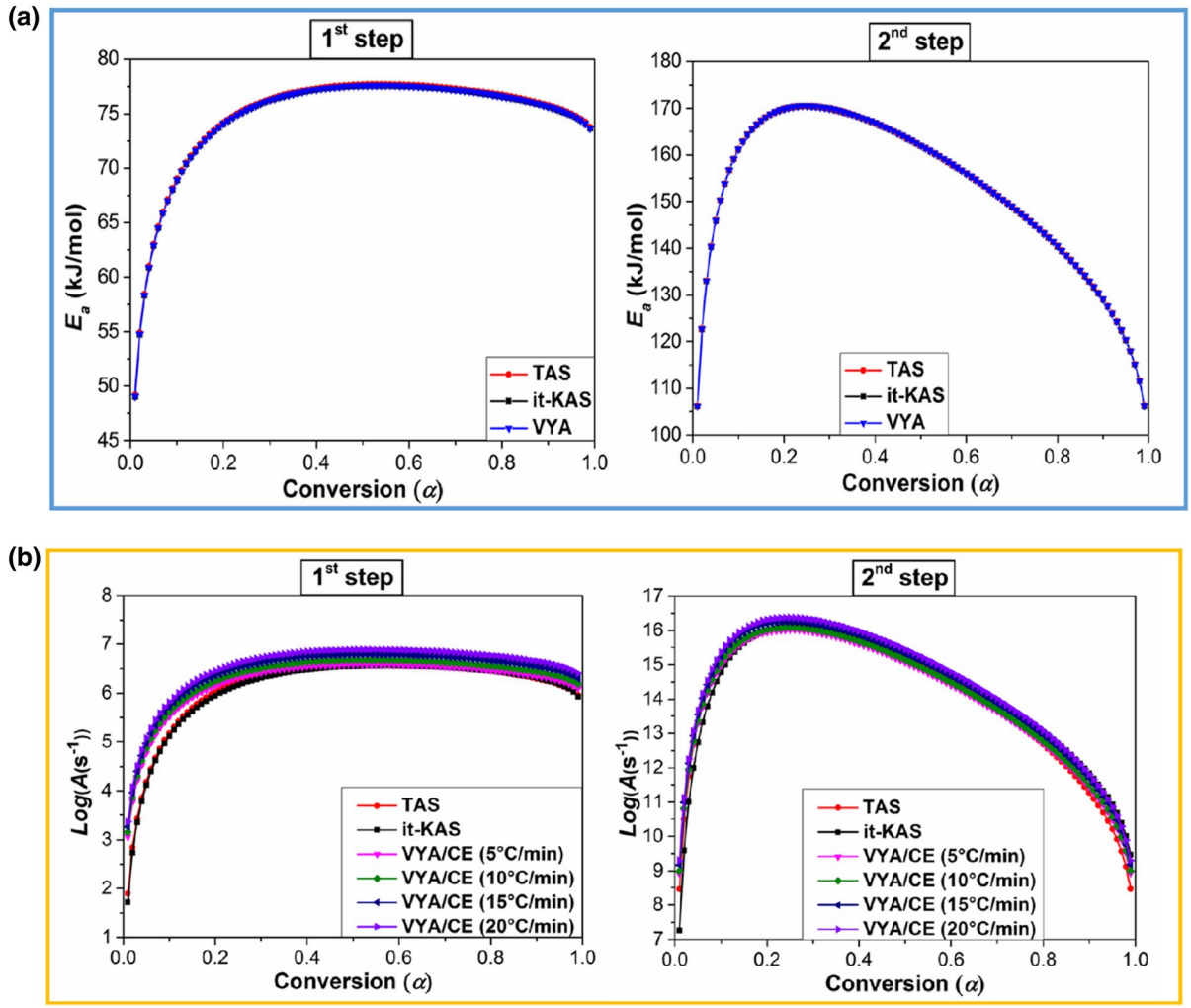

Fig. 4 **a** Variation of the Activation energy and **b** Decimal logarithm of the Pre-exponential factor with the extent of conversion for each decomposition step of NCS

Table 3 Kinetic triplet for the thermal decomposition of energetic NCS and NC biopolymers determined by isoconversional methods

Sample	Isoconversional method	$E\alpha$ (kJ/mol)	$Log(A(s^{-1}))$	g(α)
NCS 1st step	TAS	74.7 ± 3.1	6.11 ± 0.35	$F_{1/2}=1-(1-\alpha)^{1/2}$
	it-KAS	74.6 ± 3.2	6.08 ± 0.30	$F_{3/4}=1-(1-\alpha)^{1/4}$
	VYA/CE	74.7 ± 3.2	6.18 ± 0.27	–
			6.25 ± 0.27	–
			6.32 ± 0.27	–
			6.38 ± 0.26	–
	$\beta=5$ °C/min			
	$\beta=10$ °C/min			
	$\beta=15$ °C/min			
	$\beta=20$ °C/min			
NCS	TAS	152.6 ± 7.4	14.16 ± 1.94	$A_{2/3}=[-\ln(1-\alpha)]^{3/2}$
2nd step	it-KAS	152.5 ± 7.3	14.18 ± 1.90	$A_{2/3}=[-\ln(1-\alpha)]^{3/2}$
	VYA/CE	152.6 ± 6.2	14.05 ± 1.65	–
			14.11 ± 1.63	–
			14.25 ± 1.58	–
			14.33 ± 1.56	–
	$\beta=5$ °C/min			
	$\beta=10$ °C/min			
	$\beta=15$ °C/min			
	$\beta=20$ °C/min			
NC (Tarchoun et al. 2020a)	TAS	173 ± 8	17 ± 1	$A_2=[-\ln(1-\alpha)]^{1/2}$
	it-KAS	173 ± 8	17 ± 1	$F_{2/3}=1-(1-\alpha)^{1/3}$
	VYA/CE	172 ± 8	17 ± 2	–
			17 ± 2	–
			17 ± 3	–
			17 ± 2	–
	$\beta=5$ °C/min			
	$\beta=10$ °C/min			
	$\beta=15$ °C/min			
	$\beta=20$ °C/min			

is much faster in the earlier stage of $\alpha \leq 0.6$ and decreases at higher conversion. On the other hand, in the second decomposition event, the E_a tends to increase until reaching the highest value of 170 kJ/mol at $\alpha=0.25$, and then decreases until the end of the reaction. This profile is a characteristic of a complex multi-step process and indicates that there are several competitive mechanisms, which lead to activation energies increase and decrease. This increase of E_a, within the conversion range of 0.02–0.25, is mainly attributed to the degradation of nitrated glucosamine units, whereas the downtrends E_a is possibly due to the further destruction of the polymeric framework through autocatalytic reaction channels promoted by the released radicals and oxidizing species during the first thermolysis process. We can also denote from Fig. 4 that the evolution trend of E_a and *Log* (*A*) with respect to the conversion, for each thermolysis stage, is similar, which is attributed to the corresponding energy compensation effects during decomposition (Muravyev et al. 2019; Sbirrazzuoli 2020).

For comparison purposes, it is more appropriate to consider the average values of Arrhenius parameters. Therefore, it can reveal from Table 3 that the average activation energy and pre-exponential factor obtained

for the first thermolysis process of NCS are significantly lower than the characteristic range commonly found for conventional NC ($E\alpha$: 150–190 kJ/mol; Log (A): 12–18 s^{-1}) (Cherif et al. 2020; Cieślak et al. 2020). This finding is mainly caused by the presence of both thermally unstable O–NO_2 and N–NO_2, which accelerates the beginning of the decomposition event as outlined by TGA/DSC analyses and mentioned in previous studies (Tarchoun et al. 2020a, 2021d). Nevertheless, in the second decomposition event, the corresponding mean kinetic values become comparable to those of NC.

Another important point in the examination of the thermokinetic behavior of NCS is to estimate the most probable theoretical model of decomposition $g(\alpha)$ derived from the computed isoconversional methods. The obtained plots of $g(\alpha)$ for the two investigated processes are displayed in Fig. 5 and their mathematical formulas are listed in Table 3. It is worthy to mention that the non-linear Vyazovkin's approach coupled with the compensation effect provides only numerical values of the experimental $g(\alpha)$ model (Mianowski et al. 2021; Sbirrazzuoli 2020). According to TAS and it-KAS methods, the first decomposition process of NCS is governed by a deceleratory contracting cylinder process ($F_{1/2}$) and a chemical reaction mechanism ($F_{3/4}$), respectively. However, the same integral model for the second decomposition stage is provided by the two kinetic methods, which is an Avrami-Erofeev nucleation ($A_{2/3}$) characterized by a sigmoidal decomposition rate similar to that mostly obtained for NC (Benhammada et al. 2020; Tarchoun et al. 2022a). Based on the above thermokinetic findings, we can conclude that the designed energetic NCS biopolymer is thermally less stable in comparison to the chemical structurally similar NC. Nevertheless, its low kinetic parameters provide it with a high reactivity against thermal decomposition.

Heat of combustion and detonation parameters

For the purpose of analyzing the energetic properties of the synthesized NCS, its constant-volume energy of combustion ($\Delta_c U$) was experimentally determined using an oxygen calorimeter bomb. An interesting finding that one can reveal from Table 3 is that the heat released during the combustion of NCS is greater than that of structurally similar NC, demonstrating its promising combustion performance. It is interesting to point out that the heat of combustion of NCS prepared in this work from commercially available chitosan acquired from Acros Organics is found to be higher than that previously published ($7832 \leq -\Delta_c U$ (J/g) ≤ 9721) (Li et al. 2020), which is probably due to the origin of the starting chitosan biopolymer, its preliminary processing, and nitration conditions. The standard molar enthalpy of formation ($\Delta_f H$) of NCS was then calculated based on combustion reaction, along with Hess's Law and known standard enthalpies of formation of water (− 286 kJ/mol) and carbon

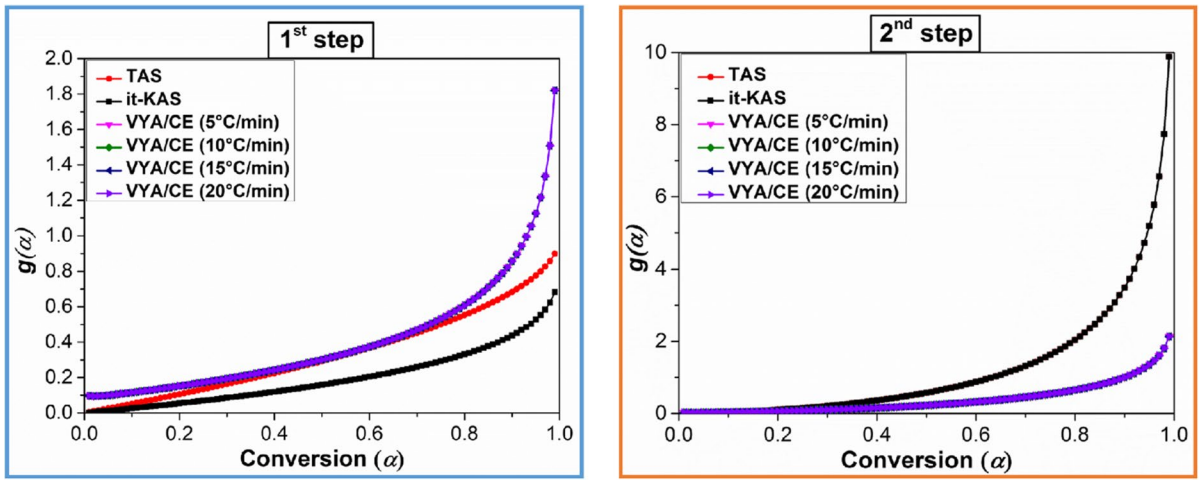

Fig. 5 Variation of the most probable integral reaction model as a function of conversion for each thermal decomposition step of NCS

dioxide (− 394 kJ/mol). It is obvious from Table 4 that NCS has a negative $\Delta_f H$, which indicates the exothermic reaction of formation of this energetic polysaccharide and its higher stability compared to the basic reagents used to form it.

The EXPLO5 V6.04 software was subsequently used to compute the detonation energy, velocity, temperature, and pressure of the investigated energetic NCS, and the obtained data are summarized in Table 4. To our best knowledge, this is the first time that the energetic properties of NCS have been reliably predicted according to the Chapman-Jouguet (CJ) theory using the above-mentioned thermodynamic computer code. Interestingly, NCS shows higher heat of explosion and detonation velocity than the state of the art reported NC and GAP, which are even superior to those of some new designed energetic polymers, such as glycidyl nitramine polymer ($\Delta_E U^0$= 4813 kJ/kg and D_{C-J}=7165 m/s) (Betzler et al. 2016), nitrated ethylenediamine-functionalized cellulose ($\Delta_E U^0$= 4774 kJ/kg and D_{C-J}=7576 m/s) (Tarchoun et al. 2020c), 2-(1H-tetrazol-5-yl)acetate cellulose nitrate ($\Delta_E U^0$=4574 kJ/kg and D_{C-J}=7522 m/s) (Tarchoun et al. 2020b), and other energetic polymeric materials recently developed by Wu et al. (Wu et al. 2020). In addition, it is noteworthy that the performance of NCS is also higher than those of some explosives including TNT (D_{C-J}=6881 m/s) (Tang et al. 2020), and HNS (D_{C-J}=6830 m/s) (Suceska et al. 2021), but lower than those of RDX (D_{C-J}=8801 m/s) (Lenz et al. 2021), HMX (D_{C-J}=8920 m/s) (Suceska et al. 2021), and PETN (D_{C-J}=8369 m/s) (Born et al. 2021). Additionally, the specific impulse (I_{sp}) of the designed energetic NCS was also calculated under isobaric conditions at 7 MPa by using EXPLO5 (V6.04) program. It should be noted that I_{sp} is widely determined to evaluate the efficiency of rocket boosters. Therefore, a propellant with a high I_{sp} is more powerful as it produces more thrust per unit of propellants. The computational results reported in Table 4 show that NCS has an interesting specific impulse of 244 s, which is greater than that of the currently used energetic binders, including NC (239 s) (Tarchoun et al. 2020d), and GAP (207 s) (Betzler et al. 2016). These outcomes reveals the improved energetic strengthens of NCS and demonstrates its significant real-word potential application in energetic formulations.

Conclusion

In the present work, a highly energetic nitrogen-rich polysaccharide was successfully synthesized through an efficient nitration process of commercially available chitosan. Interestingly, NCS's nitrogen content and density are found to be better than those of the conventional NC, and its impact sensitivity is similar to that of TNT. The high purity of the designed NCS was confirmed by FTIR analysis, SEM micrographs revealed its granular structure shape, while thermal analysis using TGA and DSC showed its two consecutive decomposition steps with lower thermal stability but much greater heat release than the common NC. More importantly,

Table 4 Combustion parameters and calculated detonation performance

	NCS	NC (Tarchoun et al. 2020d)	GAP (Betzler et al. 2016)	TNT (Tang et al. 2020)	RDX (Lenz et al. 2021)
Formula (repeating unit)	$C_{5.89}H_{7.95}N_{3.40}O_{9.83}$	$C_{6.01}H_{7.10}N_{2.63}O_{10.90}$	$C_3H_5N_3O$	$C_7H_5N_3O_6$	$C_6H_6N_6O_6$
$\Delta_c U^a$(J/g)	− 10,573	− 9226	–	–	–
$\Delta_c H^b$(kJ/mol)	− 2986	− 2669	–	–	–
$\Delta_f H^c$(kJ/mol)	− 472	− 714	142	− 355	31
Values predicted by EXPLO5 V6.04					
$-\Delta_E U^{0d}$(kJ/kg)	5151	4734	4307	–	5740
D_{C-J}^e(m/s)	7788	7456	6638	6881	8801
T_{C-J}^f(K)	3435	3412	2404	–	3745
P_{C-J}^g(GPa)	24	23	12.9	19.5	33.6
I_{sp}^h(s)	244	239	207	–	–

[a] Experimental energy of combustion; [b] Experimental molar enthalpy of combustion; [c] Calculated molar enthalpy of formation; [d] energy of explosion; [e] Detonation velocity; [f] explosion temperature; [g] Detonation pressure; [h] Specific impulse

we gave the first example of the thermokinetic behavior of the as-prepared NCS using three-isoconversional integral approaches. The predicted kinetic parameters of the deconvoluted DSC peaks of NCS's decomposition demonstrated its high reactivity with apparent activation energies of 74 kJ/mol and 152 kJ/mol for the first and second events, respectively. In addition, the computational energetic performance using Explo5 (V6.04) software highlighted the improved detonation properties and a specific impulse of NCS. Above all, energetic NCS shows the great potential to be utilized as a promising energetic nitrogen-rich biopolymer for future high-performance formulations, including composite explosives and solid propellants. Besides that, this research provides helpful guidelines for the development of a new generation of energetic materials based on polysaccharides and opens up new frontiers of research in the energetic field.

Acknowledgments Financial support of this research by the Ecole Militaire Polytechnique is gratefully acknowledged. We also thank Dr. Fodil Cherif and Dr. Sabri Touidjine for their dedicated help regarding SEM measurements and sensitivity tests.

Authors' contributions The article was written with the contributions of all authors. All authors have approved the final version of the article.

Funding The authors declare that they have received no specific grant from any funding agency in the public, commercial, or not-for-profit sectors.

Data availability All data supporting the findings of this study are available within the article.

Declarations

Conflict of interest The authors declare that they have no conflicts of interest with respect to the research, authorship, and/or publication of this article.

Informed consent Informed consent was obtained from all individual participants included in the study.

Human or animal rights This article does not contain any studies with human participants or animals performed by any of the authors.

References

Ahmad M, Ren J, Zhang Y, Kou H, Zhang Q, Zhang B (2022) Simple and facile preparation of tunable chitosan tubular nanocomposite microspheres for fast uranium (VI) removal from seawater. Chem Eng J 427:130934. https://doi.org/10.1016/j.cej.2021.130934

Ambekar A, Yoh JJ (2018) Kinetics deconvolution study of multi-component pyrotechnics. Thermochim Acta 667:27–34. https://doi.org/10.1016/j.tca.2018.07.007

Bakshi PS, Selvakumar D, Kadirvelu K, Kumar N (2020) Chitosan as an environment friendly biomaterial–a review on recent modifications and applications. Int J Biol Macromol 150:1072–1083. https://doi.org/10.1016/j.ijbiomac.2019.10.113

Barbosa HF, Francisco DS, Ferreira AP, Cavalheiro ÉT (2019) A new look towards the thermal decomposition of chitins and chitosans with different degrees of deacetylation by coupled TG-FTIR. Carbohyd Polym 225:115232. https://doi.org/10.1016/j.carbpol.2019.115232

Bekhouche S, Trache D, Abdelaziz A, Fouzi Tarchoun A, Chelouche S, Benchaa W, Belgacemi R (2021) Insight into the effect of moisture and thermal aging on the degradation of a pyrotechnic igniter composition through thermogravimetric kinetics coupled with deconvolution approach. ChemistrySelect 6:14060–14070. https://doi.org/10.1002/slct.202103758

Benhammada A, Trache D, Kesraoui M, Tarchoun AF, Chelouche S, Mezroua A (2020) Synthesis and characterization of α-Fe2O3 nanoparticles from different precursors and their catalytic effect on the thermal decomposition of nitrocellulose. Thermochim Acta 686:178570. https://doi.org/10.1016/j.tca.2020.178570

Betzler FM, Hartdegen VA, Klapötke TM, Sproll SM (2016) A new energetic binder: glycidyl nitramine polymer. Cent Eur J Energ Mat 13:289–300

Blilid S et al (2020) Phosphorylated Micro-and Nanocellulose-filled chitosan nanocomposites as fully sustainable, biologically active bioplastics. ACS Sustain Chem Eng 8:18354–18365. https://doi.org/10.1021/acssuschemeng.0c04426

Born M, Fessard TC, Göttemann L, Klapötke TM, Stierstorfer J, Voggenreiter M (2021) 3, 3-Dinitratooxetane–an important leap towards energetic oxygen-rich monomers and polymers. Cheml Commun 57:2804–2807. https://doi.org/10.1039/D1CC00466B

Chelouche S, Trache D, Tarchoun AF, Abdelaziz A, Khimeche K, Mezroua A (2019) Organic eutectic mixture as efficient stabilizer for nitrocellulose: kinetic modeling and stability assessment. Thermochim Acta 673:78–91. https://doi.org/10.1016/j.tca.2019.01.015

Cherif MF, Trache D, Benaliouche F, Tarchoun AF, Chelouche S, Mezroua A (2020) Organosolv lignins as new stabilizers for cellulose nitrate: thermal behavior and stability assessment. Int J Biol Macromol 164:794–807. https://doi.org/10.1016/j.ijbiomac.2020.07.024

Cieślak K, Gańczyk-Specjalska K, Drożdżewska-Szymańska K, Uszyński M (2020) Effect of stabilizers and nitrogen content on thermal properties of nitrocellulose granules. J Therm Anal Calorim 143:3459–3470. https://doi.org/10.1007/s10973-020-09304-8

da Silva Lucas AJ, Oreste EQ, Costa HLG, Lopez HM, Saad CDM, Prentice C (2021) Extraction, physicochemical characterization, and morphological properties of chitin and chitosan from cuticles of edible insects. Food Chem

343:128550. https://doi.org/10.1016/j.foodchem.2020.128550
Dobrynin OS et al (2019) Supercritical antisolvent processing of nitrocellulose: downscaling to nanosize, reducing friction sensitivity and introducing burning rate catalyst. Nanomaterials 9:1386. https://doi.org/10.3390/nano9101386
El Hazzat M, Sifou A, Arsalane S, El Hamidi A (2020) Novel approach to thermal degradation kinetics of gypsum: application of peak deconvolution and model-free isoconversional method. J Therm Anal Calorim 140:657–671. https://doi.org/10.1007/s10973-019-08885-3
Farkas C et al (2020) Application of chitosan-based particles for deinking of printed paper and its bioethanol fermentation. Fuel 280:118570. https://doi.org/10.1016/j.fuel.2020.118570
Hirano S, Yano H (1986) Some nitrated derivatives of N-acylchitosan. Int J Biol Macromol 8:153–156. https://doi.org/10.1016/0141-8130(86)90018-8
Hu M et al (2016) Thermogravimetric kinetics of lignocellulosic biomass slow pyrolysis using distributed activation energy model, Fraser-Suzuki deconvolution, and isoconversional method. Energ Convers Manage 118:1–11. https://doi.org/10.1016/j.enconman.2016.03.058
Huang A-C, Huang C-F, Xing Z-X, Jiang J-C, Shu C-M (2019) Thermal hazard assessment of the thermal stability of acne cosmeceutical therapy using advanced calorimetry technology. Process Saf Envion 131:197–204. https://doi.org/10.1016/j.psep.2019.09.016
Huang A-C, Huang C-F, Tang Y, Xing Z-X, Jiang J-C (2021a) Evaluation of multiple reactions in dilute benzoyl peroxide concentrations with additives using calorimetric technology. J Loss Prevent Proc 69:104373. https://doi.org/10.1016/j.jlp.2020.104373
Huang A-C et al (2021b) Calorimetric approach to establishing thermokinetics for cosmeceutical benzoyl peroxides containing metal ions. J Therm Anal Calorim 144:373–382. https://doi.org/10.1007/s10973-021-10703-8
Huet G, Hadad C, González-Domínguez JM, Courty M, Jamali A, Cailleu D, van Nhien AN (2021) IL versus DES: Impact on chitin pretreatment to afford high quality and highly functionalizable chitosan. Carbohyd Polym 269:118332. https://doi.org/10.1016/j.carbpol.2021.118332
Jha PK, Halada GP, McLennan SM (2013) Electrochemical synthesis of nitro-chitosan and its performance in chromium removal. Coatings 3:140–152. https://doi.org/10.3390/coatings3030140
Joseph SM, Krishnamoorthy S, Paranthaman R, Moses J, Anandharamakrishnan C (2021) A review on source-specific chemistry, functionality, and applications of chitin and chitosan. Carbohyd Polym Technolog Appl 2:100036. https://doi.org/10.1016/j.carpta.2021.100036
Kahdestani SA, Shahriari MH, Abdouss M (2021) Synthesis and characterization of chitosan nanoparticles containing teicoplanin using sol–gel. Polym Bull 78:1133–1148. https://doi.org/10.1007/s00289-020-03134-2
Kaya M et al (2018) Antioxidative and antimicrobial edible chitosan films blended with stem, leaf and seed extracts of Pistacia terebinthus for active food packaging. RSC Adv 8:3941–3950. https://doi.org/10.1039/C7RA12070B
Lenz T, Klapötke TM, Mühlemann M, Stierstorfer J (2021) About the azido derivatives of pentaerythritol tetranitrate. Propell Explos Pyrot 46:723–731. https://doi.org/10.1002/prep.202000265
Li C, Li H, Xu K (2020) High-substitute nitrochitosan used as energetic materials: preparation and detonation properties. Carbohyd Polym 237:116176. https://doi.org/10.1016/j.carbpol.2020.116176
Li Z-P et al (2021) Thermal hazard evaluation on spontaneous combustion characteristics of nitrocellulose solution under different atmospheric conditions. Sci Rep 11:1–13. https://doi.org/10.1038/s41598-021-03579-z
Li Z-P, Huang A-C, Tang Y, Zhou H-L, Liu Y-C, Huang C-F, Shu C-M, Xing Z-X, Jiang J-C (2022) Thermokinetic prediction and safety evaluation for toluene sulfonation process and product using calorimetric technology. J Therm Anal Calorim. https://doi.org/10.1007/s10973-022-11384-7
Liu Y-C et al (2022) Hazard assessment of the thermal stability of nitrification by-products by using an advanced kinetic model. Process Saf Envion 160:91–101. https://doi.org/10.1016/j.psep.2022.02.004
Mauricio-Sánchez RA, Salazar R, Luna-Bárcenas JG, Mendoza-Galván A (2018) FTIR spectroscopy studies on the spontaneous neutralization of chitosan acetate films by moisture conditioning. Vib Spectrosc 94:1–6. https://doi.org/10.1016/j.vibspec.2017.10.005
Mianowski A, Radko T, Siudyga T (2021) Kinetic compensation effect of isoconversional methods. React Kinet Mech Cat 132:37–58. https://doi.org/10.1007/s11144-020-01898-2
Min BS, Park YC (2009) A study on the aliphatic energetic plasticizers containing nitrate ester and nitramine. J Ind Eng Chem 15:595–601. https://doi.org/10.1016/j.jiec.2009.01.017
Mohammed ASA, Naveed M, Jost N (2021) Polysaccharides; classification, chemical properties, and future perspective applications in fields of pharmacology and biological medicine (a review of current applications and upcoming potentialities). J Polym Environ 29:2359–2371. https://doi.org/10.1007/s10924-021-02052-2
Mohan K et al (2020) Recent insights into the extraction, characterization, and bioactivities of chitin and chitosan from insects. Trends Food Sci Technol 105:17–42. https://doi.org/10.1016/j.tifs.2020.08.016
Mujtaba M et al (2020) Chitosan-based delivery systems for plants: a brief overview of recent advances and future directions. Int J Biol Macromol 154:683–697. https://doi.org/10.1016/j.ijbiomac.2020.03.128
Muravyev NV, Pivkina AN, Koga N (2019) Critical appraisal of kinetic calculation methods applied to overlapping multistep reactions. Molecules 24:2298. https://doi.org/10.3390/molecules24122298
Nasrollahzadeh M, Sajjadi M, Iravani S, Varma RS (2021) Starch, cellulose, pectin, gum, alginate, chitin and chitosan derived (nano) materials for sustainable water treatment: A review. Carbohyd Polym 251:116986. https://doi.org/10.1016/j.carbpol.2020.116986
Negm NA, Hefni HH, Abd-Elaal AA, Badr EA, Abou Kana MT (2020) Advancement on modification of chitosan biopolymer and its potential applications. Int J Biol

Macromol 152:681–702. https://doi.org/10.1016/j.ijbiomac.2020.02.196
Nikolsky SN, Zlenko DV, Melnikov VP, Stovbun SV (2019) The fibrils untwisting limits the rate of cellulose nitration process. Carbohyd Polym 204:232–237. https://doi.org/10.1016/j.carbpol.2018.10.019
Oladzadabbasabadi N, Nafchi AM, Ariffin F, Wijekoon MJO, Al-Hassan A, Dheyab MA, Ghasemlou M (2022) Recent advances in extraction, modification, and application of chitosan in packaging industry. Carbohyd Polym 277:118876. https://doi.org/10.1016/j.carbpol.2021.118876
Peter S, Lyczko N, Gopakumar D, Maria HJ, Nzihou A, Thomas S (2021) Chitin and chitosan based composites for energy and environmental applications: a review. Waste Biomass Valori 12:4777–4804. https://doi.org/10.1007/s12649-020-01244-6
Pinto RJ et al (2021) Cellulose nanocrystals/chitosan-based nanosystems: synthesis, characterization, and cellular uptake on breast cancer cells. Nanomaterials 11:2057. https://doi.org/10.3390/nano11082057
Poli M, Rahman N, Hanifah S, Zani A, Ahmad A (2015) Modification of chitosan for preparation of poly (N-isopropylacrylamide/O-nitrochitosan) interpenetrating polymer network. Sains Malays 44:995–1001
Rabiee N, Bagherzadeh M, Tavakolizadeh M, Pourjavadi A, Atarod M, Webster TJ (2022) Synthesis, characterization and mechanistic study of nano chitosan tetrazole as a novel and promising platform for CRISPR delivery. Int J Polym Mater Polym 71:116–126. https://doi.org/10.1080/00914037.2020.1809405
Rahman NA, Abu Hanifah S, Mobarak NN, Su'ait MS, Ahmad A, Shyuan LK, Khoon LT (2019) Synthesis and characterizations of o-nitrochitosan based biopolymer electrolyte for electrochemical devices. PloS one 14:e0212066. https://doi.org/10.1371/journal.pone.0212066
Rasweefali M, Sabu S, Sunooj K, Sasidharan A, Xavier KM (2021) Consequences of chemical deacetylation on physicochemical, structural and functional characteristics of chitosan extracted from deep-sea mud shrimp. Carbohyd Polym Technolog Appl 2:100032. https://doi.org/10.1016/j.carpta.2020.100032
Reshmy R et al (2022) Lignocellulose in future biorefineries: strategies for cost-effective production of biomaterials and bioenergy. Bioresource Technol 344:126241. https://doi.org/10.1016/j.biortech.2021.126241
Rezaei FS, Sharifianjazi F, Esmaeilkhanian A, Salehi E (2021) Chitosan films and scaffolds for regenerative medicine applications: a review. Carbohyd Polym 273:118631. https://doi.org/10.1016/j.carbpol.2021.118631
Sbirrazzuoli N (2020) Determination of pre-exponential factor and reaction mechanism in a model-free way. Thermochim Acta 691:178707. https://doi.org/10.1016/j.tca.2020.178707
Sivanesan I, Gopal J, Muthu M, Shin J, Mari S, Oh J (2021) Green synthesized chitosan/chitosan nanoforms/nanocomposites for drug delivery applications. Polymers 13:2256. https://doi.org/10.3390/polym13142256
Suceska M, Dobrilovic M, Bohanek V, Stimac B (2021) Estimation of explosive energy output by EXPLO5 thermochemical code. Z Anog Allg Chem 647:231–238. https://doi.org/10.1002/zaac.202000219
Sućeska M (2017) EXPLO5 V6. 04, Brodarski Institute, Zagreb
Tang J, Yang P, Yang H, Xiong H, Hu W, Cheng G (2020) A simple and efficient method to synthesize high-nitrogen compounds: incorporation of tetrazole derivatives with N5 chains. Chem Eng J 386:124027. https://doi.org/10.1016/j.cej.2020.124027
Tarchoun AF, Trache D, Klapötke TM, Belmerabet M, Abdelaziz A, Derradji M, Belgacemi R (2020a) Synthesis, characterization, and thermal decomposition kinetics of nitrogen-rich energetic biopolymers from aminated giant reed cellulosic fibers. Ind Eng Chem Res 59:22677–22689. https://doi.org/10.1021/acs.iecr.0c05448
Tarchoun AF, Trache D, Klapötke TM, Khimeche K (2020b) Tetrazole-functionalized microcrystalline cellulose: A promising biopolymer for advanced energetic materials. Chem Eng J 400:125960. https://doi.org/10.1016/j.cej.2020.125960
Tarchoun AF, Trache D, Klapötke TM, Krumm B (2020c) New insensitive nitrogen-rich energetic polymers based on amino-functionalized cellulose and microcrystalline cellulose: synthesis and characterization. Fuel 277:118258. https://doi.org/10.1016/j.fuel.2020.118258
Tarchoun AF, Trache D, Klapötke TM, Krumm B, Khimeche K, Mezroua A (2020d) A promising energetic biopolymer based on azide-functionalized microcrystalline cellulose: synthesis and characterization. Carbohyd Polym 249:116820. https://doi.org/10.1016/j.carbpol.2020.116820
Tarchoun AF, Trache D, Klapötke TM, Abdelaziz A, Derradji M, Bekhouche S (2021a) Chemical design and characterization of cellulosic derivatives containing high-nitrogen functional groups: Towards the next generation of energetic biopolymers. Defence Technol 18:537–546. https://doi.org/10.1016/j.dt.2021.03.009
Tarchoun AF, Trache D, Klapötke TM, Krumm B, Kofen M (2021b) Synthesis and characterization of new insensitive and high-energy dense cellulosic biopolymers. Fuel 292:120347. https://doi.org/10.1016/j.fuel.2021.120347
Tarchoun AF, Trache D, Klapötke TM, Krumm B, Mezroua A, Derradji M, Bessa W (2021c) Design and characterization of new advanced energetic biopolymers based on surface functionalized cellulosic materials. Cellulose 28:6107–6123. https://doi.org/10.1007/s10570-021-03965-w
Tarchoun AF et al (2021d) New insensitive high-energy dense biopolymers from giant reed cellulosic fibers: their synthesis, characterization, and non-isothermal decomposition kinetics. New J Chem 45:5099–5113. https://doi.org/10.1039/D0NJ05484D
Tarchoun AF, Sayah ZBD, Trache D, Klapötke TM, Belmerabt M, Abdelaziz A, Bekhouche S (2022a) Towards investigating the characteristics and thermal kinetic behavior of emergent nanostructured nitrocellulose prepared using various sulfonitric media. J Nanostruct Chem. https://doi.org/10.1007/s40097-021-00466-x
Tarchoun AF, Trache D, Klapötke TM, Abdelaziz A, Bekhouche S, Boukeciat H, Sahnoun N (2022b) Making progress towards promising energetic cellulosic microcrystals developed from alternative lignocellulosic biomasses.

J Energ Mater. https://doi.org/10.1080/07370652.2022.2032484

Tarchoun AF et al (2022c) Valorization of esparto grass cellulosic derivatives for the development of promising energetic azidodeoxy biopolymers: synthesis, characterization and isoconversional thermal kinetic analysis. Propell Explos Pyrot 47:e202100293. https://doi.org/10.1002/prep.202100293

Trache D, Tarchoun AF (2019) Differentiation of stabilized nitrocellulose during artificial aging: spectroscopy methods coupled with principal component analysis. J Chemometr 33:e3163. https://doi.org/10.1002/cem.3163

Trache D, Abdelaziz A, Siouani B (2017) A simple and linear isoconversional method to determine the pre-exponential factors and the mathematical reaction mechanism functions. J Therm Anal Calorim 128:335–348. https://doi.org/10.1007/s10973-016-5962-0

Trache D, Maggi F, Palmucci I, DeLuca LT (2018) Thermal behavior and decomposition kinetics of composite solid propellants in the presence of amide burning rate suppressants. J Therm Anal Calorim 132:1601–1615. https://doi.org/10.1007/s10973-018-7160-8

UN-TDG, UN (2009) Recommendations on the transport of dangerous goods: manual of tests and criteria. United Nations Publications, New York UN

Vyazovkin S, Burnham AK, Favergeon L, Koga N, Moukhina E, Pérez-Maqueda LA, Sbirrazzuoli N (2020) ICTAC Kinetics committee recommendations for analysis of multi-step kinetics. Thermochim Acta 689:178597. https://doi.org/10.1016/j.tca.2020.178597

Wang B, Feng Y, Qi X, Deng M, Tian J, Zhang Q (2018) Designing explosive poly (ionic liquid) s as novel energetic polymers. Chem Eur J 24:15897–15902. https://doi.org/10.1002/chem.201803159

Wei R, Huang S, Weng J, Wang J, Wang C (2021) Comparative analysis of stable decomposition and combustion kinetics of nitrated cellulose. Cellulose 28:9613–9632. https://doi.org/10.1007/s10570-021-04162-5

Wu Q, Ma Q, Zhang Z, Yang W, Gou S, Huang J, Fan G (2020) Combustion and catalytic performance of metal-free heat-resistant energetic polymeric materials. Chem Eng J 399:125739. https://doi.org/10.1016/j.cej.2020.125739

Yan Q-L, Cohen A, Chinnam AK, Petrutik N, Shlomovich A, Burstein L, Gozin M (2016) A layered 2D triaminoguanidine–glyoxal polymer and its transition metal complexes as novel insensitive energetic nanomaterials. J Mater Chem A 4:18401–18408. https://doi.org/10.1039/C6TA08041C

Yin Z, Chu R, Zhu L, Li S, Mo F, Hu D, Liu C (2021) Application of chitosan-based flocculants to harvest microalgal biomass for biofuel production: a review. Renew Sustain Energ Rev 145:111159. https://doi.org/10.1016/j.rser.2021.111159

Zeng M, Zhang L, Kennedy JF (2005) Intermolecular interaction and properties of cross-linked materials from poly (ester-urethane) and nitrochitosan. Carbohyd Polym 60:399–409. https://doi.org/10.1016/j.carbpol.2005.02.002

Zhang W, Qin Z, Yi J, Chen S, Xu K (2022) Laser ignition and combustion properties of composite with high-substituted nitrochitosan and nano-Ti powder. Combust Flame 240:112056. https://doi.org/10.1016/j.combustflame.2022.112056

Zhou H-L et al (2022) Calorimetric evaluation of thermal stability and runaway hazard based on thermokinetic parameters of O, O–dimethyl phosphoramidothioate. J Loss Prevent Proc 75:104697. https://doi.org/10.1016/j.jlp.2021.104697